Progression to Islet Destruction in a Cyclophosphamide-Induced Transgenic Model

A Microarray Overview

Michael Matos,[1,2] Richard Park,[1] Diane Mathis,[1] and Christophe Benoist[1]

Type 1 diabetes appears to progress not as an uncontrolled autoimmune attack on the pancreatic islet β-cells, but rather in a highly regulated manner. Leukocytic infiltration of the pancreatic islets by autoimmune cells, or insulitis, can persist for long periods of time before the terminal destruction of β-cells. To gain insight on the final stage of diabetogenesis, we have studied progression to diabetes in a $CD4^+$ T-cell receptor transgenic variant of the NOD mouse model, in which diabetes can be synchronously induced within days by a single injection of cyclophosphamide. A time-course analysis of the gene expression profiles of purified islets was performed using microarrays. Contrary to expectations, changes in transcripts subsequent to drug treatment did not reflect a perturbation of gene expression in $CD4^+$ T-cells or a reduction in the expression of genes characteristic of regulatory T-cell populations. Instead, there was a marked decrease in transcripts of genes specific to B-cells, followed by an increase in transcripts of chemokine genes (cxcl1, cxcl5, and ccl7) and of other genes typical of the myelo-monocytic lineages. Interferon-γ dominated the changes in gene expression to a striking degree, because close to one-half of the induced transcripts issued from interferon-γ–regulated genes. *Diabetes* 53:2310–2321, 2004

The nonobese diabetic (NOD) mouse, discovered in the 1970s, has been a commonly used model of human type 1 diabetes. As in humans, disease progresses in these mice in at least two definable stages. In a first stage, infiltration of autoreactive cells into the pancreatic islets begins after 4 weeks of age and becomes progressively more extensive, but spares a proportion of insulin-producing β-cells. This pre-diabetic state can persist for months (years in patients), the autoimmune attack remaining controlled and relatively nondestructive (although our perspective on the exact nature of the pre-diabetic lesion is far less precise for human patients than for mice). In a second stage, typically between 15 and 25 weeks of age in NOD mice, unknown events provoke the innocuous insulitis to progress to active β-cell destruction. Although the NOD mouse provides a performant diabetes model, disease is still very complex in these animals, with intricate genetic determinism. Disease pathogenesis likely involves a defect in central tolerance induction as well as faulty immunoregulatory cells or molecules. Evidence for the involvement of multiple antigens, lymphocyte populations, and final effector mechanisms has lead researchers to investigate simpler models.

Transgenic mouse lines have been exploited to elucidate this complexity. In several such lines, the expression of a transgene-encoded, prearranged T-cell receptor (TCR) gene confers on a majority of T-cells reactivity to an islet β-cell antigen presented by either a major histocompatibility complex (MHC) class I or class II molecule (1–4). These lines bypass the early steps of breakdown of tolerance and amplification of the autoimmune repertoire and allow the analysis of peripheral effector and regulatory mechanisms. Among these transgenic models is the BDC2.5 TCR transgenic line, derived from a diabetogenic $CD4^+$ T-cell clone (3,5). The dominant $CD4^+$ T-cells are restricted by the MHC class II Ag^7 molecule and are specific for an unidentified antigen derived from β-cell granules. BDC2.5 mice develop insulitis between 2 and 3 weeks of age, with very extensive infiltration of essentially all islets by 4 weeks. However, progression to overt diabetes is under tight control; on the NOD background, BDC2.5 animals develop diabetes only 5–15% of the time.

The state of balanced and benign insulitis can be disrupted by a number of perturbations, e.g., blockade of costimulatory molecules in the initial phase of autoreactive T-cell activation (6–8), triggering of toll-like receptors by lipopolysaccharide administration (9), apoptosis of pancreatic cells due to viral infection (10). All of these perturbations provoke an aggressive form of insulitis in BDC2.5/NOD mice that leads to destruction of β-cells and diabetes within days. Similarly, the cytotoxic drug cyclophosphamide (CY) induces diabetes within 5–7 days after injection into young adult BDC2.5/NOD mice (11). CY has been known for quite some time to accelerate diabetes in NOD mice as well, but less efficiently and over a more

From the [1]Section on Immunology and Immunogenetics, Joslin Diabetes Center, Department of Medicine, Brigham and Women's Hospital, Harvard Medical School, Boston, Massachusetts; and the [2]Division of Pediatric Endocrinology, Children's Hospital, Harvard Medical School, Boston, Massachusetts.

Address correspondence and reprint requests to Diane Mathis and Christophe Benoist, Section on Immunology and Immunogenetics, Joslin Diabetes Center, 1 Joslin Place, Boston, MA 02215. E-mail: cbdm@joslin.harvard.edu.

Received for publication 11 March 2004 and accepted in revised form 26 May 2004.

Additional information for this article can be found in an online appendix at http://diabetes.diabetesjournals.org.

CY, cyclophosphamide; FPR, false-positive rate; GPDH, glycerol phosphate dehydrogenase; IFN, interferon; IL, interleukin; JDRF, Juvenile Diabetes Research Foundation; MHC, major histocompatibility complex; NK, natural killer; RMA, robust multiarray average; TCR, T-cell receptor; TNF, tumor necrosis factor.

protracted course (12–14). In BDC2.5/NOD mice, no changes are histologically visible in the first 2 days after CY treatment; by 3 days, the fairly innocuous appearance of the insulitic lesion begins to be perturbed, and by 5 days, the lesion has become "explosive," with extensive dilacerations of the endocrine tissue and cell apoptosis. These studies demonstrated no striking changes in the proportions of the different cell populations infiltrating the islets, arguing rather for the activation of preexisting infiltrating cells.

How CY achieves destabilization of the local immunoregulatory balance is not known. The literature repeatedly invokes an effect of CY on suppressor cells, but primary data supporting this notion are hard to find. It is also not clear which cell or cells are the targets of the CY induction process. Does this cytotoxic drug primarily affect the islet β-cell, releasing intracellular contents and increasing the local autoantigen load? Or does it activate myeloid or lymphoid cells in the infiltrate?

Because of its very rapid and synchronous nature, the induction of diabetes in BDC2.5/NOD mice affords the possibility of investigating, in a highly controlled manner, the molecular and cellular events that accompany conversion to an aggressive insulitis and the accompanying diabetogenic decompensation. In earlier studies (11), we focused on cellular and histological changes that take place. Here, we have studied the unfolding of events during CY-induced diabetes by monitoring the time course of gene expression changes via microarray analysis. The aim was to determine whether, in a broad analysis of gene expression changes, one might be able to discern a signature of the programmatic changes taking place during the early phases of diabetes induction.

RESEARCH DESIGN AND METHODS

The BDC2.5/NOD transgenic line has been described previously (3). The mice used in the present experiments were from >25 backcrosses to the NOD/Lt genetic background and were all 6–8 weeks of age and nondiabetic. Both male and female mice were used. Diabetes was induced by an intraperitoneal injection of a single dose of CY (200 mg/kg in PBS).

Islet isolation. Islets were isolated by the Islet Preparation Core of the Juvenile Diabetes Research Foundation (JDRF) Center for Islet Transplantation at Harvard using a standard technique (15). Briefly, ice-cold collagenase (Liberase; Roche) was infused into the common bile duct of an anesthetized mouse. The pancreas was then removed and incubated at 37°C for ~20 min with gentle agitation. Further separation was accomplished with a Histopaque density gradient (Histopaque-1077; Sigma). The islets were handpicked under a stereomicroscope to ensure a pure islet preparation. Total RNA was isolated from these islets using Trizol followed by ethanol precipitation.

Conventional gene expression analysis. Before amplification of islet mRNA or to confirm the DNA chip analysis, transcripts of some genes were quantitated with quantitative real-time PCR. Amplification of specific genes was monitored during the PCR utilizing an internal fluorescent probe on an ABI Prism 7700 Sequence Detection System (Applied Biosystems). For each gene of interest, a TaqMan primer/probe set was designed such that both the amplified fragment and the probe spanned an intron to avoid spurious amplification from genomic DNA. For gene expression analysis, cDNA was made from 100 ng of total pancreatic islet RNA in a 20-μl reverse transcriptase reaction. Six microliters of this reverse transcription product were used for triplicate 20-μl TaqMan reactions. Transcripts of the genes of interest (interleukin [IL]-18, IL-12 p40, interferon [IFN]-γ, and Cxcl9) were normalized relative to transcripts of the ubiquitous housekeeping gene glycerol phosphate dehydrogenase (GPDH). For each experiment, a standard curve was generated for every gene based on δ-Ct (the number of cycles required to generate ~50% of the maximum amount of amplified product, set during the linear phase of amplification). Normalization of the relative amounts of a gene of interest (X) from RNA from a CY-treated (cy) versus a PBS-treated (ctl) mouse were calculated as: X_{cy}/X_{ctl} (normalized) = $(X_{cy}/X_{ctl}) \times (GPDH_{ctl}/GPDH_{cy})$.

Microarray gene expression analysis. Islet RNA was amplified using a standardized protocol (MessageAmp aRNA kit; Ambion). Briefly, cDNA was synthesized from 1 μg total RNA template by reverse transcription primed by a hybrid oligonucleotide containing oligo-T and T7 RNA polymerase promoter sequences. Double-stranded DNA was then synthesized by incubation with RNase A followed by extension with polymerase I. Multiple copies of antisense RNA were then produced with T7 RNA polymerase (~100-fold amplification). This RNA was then primed with random hexamers, and the entire amplification process was repeated, producing biotinylated RNA with 10,000-fold amplification of the original mRNA. Biotinylated cRNA was then prepared with biotinylated ribonucleotides in another T7 RNA polymerase reaction (Enzo BioArray HighYield RNA Transcript Labeling Kit; Affymetrix).

Biotinylated RNA was fragmented in a proprietary Affymetrix buffer optimized to break down full-length cRNA by metal-induced hydrolysis (https://www.affymetrix.com/download/manuals/expression_print_manual.pdf). The samples were hybridized to Affymetrix MU74v2A microarray chips in an Affymetrix Fluidics Station 400 hybridizer/analyzer, with streptavidin-phycoerythrin to detect biotinylated probe. Fluorescence on the chip was quantified on an Affymetrix Fluidics Station 400 hybridizer/analyzer and digitized using an Affymetrix GeneChip Scanner with Affymetrix GeneChip operating software. The initial reads were processed through the robust multiarray average (RMA) algorithm (implemented on the Array analyzer; Insightful) for probe-level normalization. These primary values were averaged (with outlier elimination) and an approximate measure of significance calculated (Welch's approximation t test). For analysis of significance, control datasets approximating the values and variances of the real data were generated by random reshuffling of the data (random draws within rows) or as detailed in RESULTS. The raw datasets have been deposited on the GEO databank.

RESULTS AND DISCUSSION

Previous experiments have shown that the nondestructive insulitis of adult BDC2.5/NOD mice is extensive, representing two to three times the β-cell volume (3,11,16–19). This infiltrate is heterogeneous and includes large numbers of B- and T-cells, NK (natural killer) cells, macrophages, and dendritic cells. Thus, we chose to evaluate the global response to CY in the infiltrated islet as a whole, rather than in individual cells. To set the stage for the microarray analysis, we investigated the kinetics of diabetes progression after CY treatment in our current BDC2.5/NOD colony and tested RNA preparation methods over that time period. As expected from previous results (11), diabetes was induced in a highly synchronous fashion after administration of a single intraperitoneal injection of CY (200 mg/kg) (data not shown). Islets were prepared at different times after CY treatment (90–120 islets/mouse), using a conventional islet preparation technique: retrograde intraductal injection of collagenase, density gradient fractionation, and picking of isolated islets by micromanipulation. The yield of islets was similar during the first 3 days after treatment, as has been shown previously (11). This result was consistent with parallel histological analyses that demonstrated maintenance of the islet structure up to day 3, but a breakdown after that (11) (data not shown). Because the islets that remained whole and therefore could be isolated by the collagenase procedure at day 4 were likely to represent "survivors" with a delayed evolution, we limited the gene expression analysis to the first 3 days after treatment. Histological examination showed these islets to be morphologically intact and to contain β-cell islands as well as surrounding infiltrate cells. Several RNA preparation techniques were tested; the best yields were obtained with a Trizol method, and analysis by real-time quantitative PCR showed the RNA preparations to be of good quality.

In order to ensure the validity of the microarray analysis, three or four independent experiments were per-

TABLE 1
Samples used for the microarray analysis

	No CY (day 0)	CY Day 1	CY Day 2	CY Day 3
Number of independent samples	8	4	3	3
Gene-wise coefficient of variation (mean)	0.157	0.104	0.138	0.138

The number of independent RNA samples used for microarray hybridization is listed. For each experiment, pancreatic islets were prepared from one or two pooled BDC2.5/NOD mice previously treated with CY and from control untreated littermates (referred to as "day 0"). Each of these samples was used to prepare a biotin-labeled probe for hybridization to a Mu74Av2 chip. The coefficients of variation were calculated for each gene across all samples for a condition and averaged over the entire dataset.

formed at each time point (Table 1). Each experiment also included an untreated group (hereafter referred to as "day 0"). From previous experiments (11), we knew that IL-12 expression should be induced in samples from mice progressing to diabetes. We used RT-PCR to show that IL-12 p40 transcripts were indeed induced in the samples used for microarray analysis (data not shown). From all samples, RNA was prepared, with an average yield of 80 ng, and labeled probes for microarray analysis were synthesized by using biotinylated ribonucleotides in the final RNA polymerase reaction. These probes were then hybridized to Affymetrix Mu74Av2 oligonucleotide microarrays, which represent 8,063 unique genes, of which 1,935 are expressed sequence tags.

Data processing and statistical validation. Data were processed with a custom analysis package, based on Access and S-Plus software and custom-designed scripts (R.P., unpublished work). In a preliminary step, all raw datasets within a time group were plotted against each other and visually inspected. In most cases, reproducibility was good, except for two datasets that clearly departed from other replicates, likely because of contamination with exocrine tissue; these datasets were removed from further consideration. Probe-level normalization was performed with the RMA algorithm (20) from the Bioconductor site (www.bioconductor.org, implemented on the Insightful Array analyzer), which we found to yield data far less noisy than when processed with Affymetrix MAS-5 software (20) (R.P., J. Luckey, data not shown). For each time point, the set of normalized values were compared with the day 0 set, and a P value of differences was calculated by Welsh's t test. An aggregate expression value for each feature of the Mu74Av2 chip and each time point was then calculated by simple averaging. Fold changes relative to the untreated day 0 sample were calculated from these mean values. The entire datasets are available as supplemental data in an online appendix (Table S1 [at http://diabetes.diabetesjournals.org]).

Two main strategies were used to assess the significance of the observations. First, since each experiment included a control pool, the study design generated more samples in the control day 0 group than for other time points. In validation analyses, this allowed us to divide the day 0 group into two individual subgroups (four samples each), providing an internal estimation of the intragroup experimental variability. As will be detailed below, a number of changes were observed at day 3 after CY treatment. Figure 1*A* shows that the differences between the day 3 and day 0 conditions were far more numerous than those between the replicate day 0 groups. This first analysis indicated that most of the variations described below were likely to be true and not merely a consequence of experimental fluctuation. Second, randomized data groups were generated by permutation between the 18 datasets of the expression values for each gene (row-wise permutation) and were then processed following the same methods as those for the true datasets. This generated matrices of fold change and P values for the null hypothesis (no time-dependent expression changes). This randomized dataset was used in unimodal comparisons of fold-change distributions (Table 2, see below). We also took advantage of the kinetic nature of the data. While the limited number of time points precluded the utilization of sophisticated time series techniques, an apparent false-positive rate (FPR) was estimated for the genes of interest by combining the probabilities of coordinated variation in successive time points. For each gene in the real dataset, we counted the number of genes in the random dataset presenting a similar fold-change pattern (day 2 and day 3 only). For the simulation shown in Fig. 1*B*, close to 100,000 random "gene patterns" were thus queried. The vast majority of the patterns were observed quite frequently (10^4 times or more), but a few were very rare or absent from the randomly generated data. Not surprisingly, these corresponded to genes showing the greatest fold change at day 3 relative to day 0 (Fig. 1*C*). From these computations, we derived an estimate of the FPR for each gene that showed a time-dependent variation.

Variations in gene expression. As a first analysis of changes in gene expression during the unfolding of CY-induced diabetes, we counted the overall number of genes that showed a change relative to the starting (day 0) value (Table 2). Overall, the effects of CY treatment mainly became apparent at day 3 after treatment, with a distribution of fold changes that was significantly different from that of the randomized data (Table 2, last column). For instance, an aggregate of 49 genes was induced or repressed by a factor of 3 or more, whereas only five genes showed such variation in the randomized dataset. At earlier times, while some of the changes may have been significant (see below), the overall pattern did not markedly depart from that of the randomized data. Interestingly, a roughly equivalent number of genes was induced or repressed by CY, with a fairly symmetric distribution in Table 2. This indicates that the cellular or genomic changes accompanying progression to diabetes were not limited to induction responses; it was not simply that an inflammatory response developed, but the process also included the downregulation of other functions.

We then analyzed in more detail the kinetics of expression of those genes in which transcripts were clearly altered by day 3 of CY treatment (filtered as described below). Figure 2 displays the distribution of expression at each day after CY treatment, plotted in reference to the day 0 values. Genes that eventually became induced by day 3 are shown in red, and those repressed are in blue. At day 1 (Fig. 2*A*), the majority of genes in the induced set

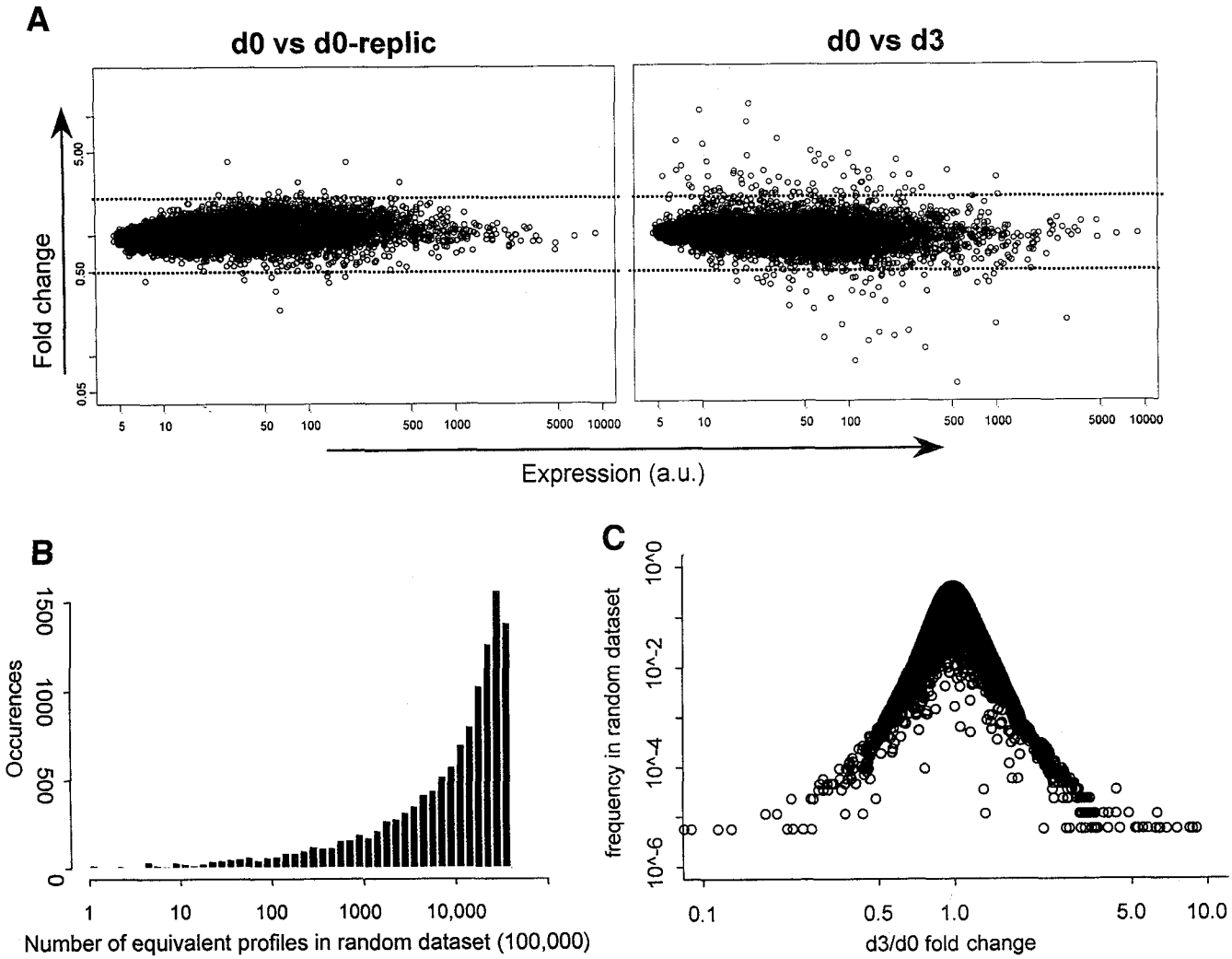

FIG. 1. Computational analysis of the microarray data. *A*: Substantial variation in gene expression 3 days after diabetes initiation by CY as assessed by Mu74Av2 microarray (RMA normalization). The plots represent the expression value (x-axis) versus the fold change relative to the day 0 (d0) value. On the left, the comparison is relative to a replicate group of day 0 samples, and day 3 (d3) values compared with day 0 are on the right. Horizontal lines indicate 2× fold change. *B* and *C*: The variations observed after CY induction are not random. *B*: Histogram representation of the number of times the observed expression patterns are reproduced in a randomized dataset generated by repeated permutation of the expression values between conditions. A few profiles are generated only very rarely or not at all by chance (<10 times per 10^5 draws). *C*: These genes of low frequency in the random dataset correspond to those exhibiting the greatest fold change.

were not yet affected, still clustering around the diagonal, except for a few repressed genes already showing a clear change. At day 2 (Fig. 2*B*), most genes in the set began to show clear differences from the day 0 values, albeit still less than the full induction seen at day 3. For the repressed gene set, a few were already underexpressed at day 1, with an amplification of the trend at day 2.

Induced genes. Fig. 3*A* presents the identity and principal expression values for the 88 genes of the "induced set." These were selected with a cutoff on fold-change values of 2.1, selected as corresponding to a univariate FPR of 20% or better. (We did not use the t test P value as a filter because the estimate of the variance used in the t test is highly unreliable when dealing with a limited number of replicates, whereas the FPR derived from simulation makes no assumptions.) The t test P value and estimated FPR are also shown for reference in Fig. 3*A*. Many of these genes exhibited a partial induction at day 2, and the combined analysis in reference to the randomized control shows that their true significance is far greater (FPRs 2.10^{-4} to 5.10^{-6}). This cutoff may eliminate from further examination a number of genes that exhibited significant, but more subtle, variations; however, they fall within a significantly more noisy range of the dataset. The following points can be made from the list in Fig. 3*A*:

Most of the changes emanated from inside the inflammatory infiltrate, rather than the islet cells themselves. The main cell type expressing each gene is indicated by color coding of the "locus link" column of the Fig., as determined by *1*) comparing relative expression in Mu74Av2 chips probed with whole-spleen or islet RNA (L. Poirot, C.B., D.M., unpublished data), from which the islet-to-spleen ratio was a clear indicator of preferential expression in pancreatic or hematopoietic cells; and *2*) retrieving information corresponding to the same chip from the GNF Gene Expression Atlas site. The majority of induced genes were typical of those transcribed by hematopoietic cells (myeloid or lymphoid, highlighted in green), and only a minority reflected responses in the target islet cells (highlighted in red). Most of these latter genes are

TABLE 2
Number of genes varying at different times after CY treatment

Fold change	Induced transcripts			Randomized datasets					
	Day 1 vs. 0	Day 2 vs. 0	Day 3 vs. 0	Day 1 vs. 0	Day 2 vs. 0	Day 3 vs. 0	Day 1 vs. 0	Day 2 vs. 0	Day 3 vs. 0
2	7	13	75	2	31	106	12	14	19
3	1	3	21	—	5	28	1	3	5
4	1	1	12	—	1	12	—	1	1
5	1	1	11	—	—	8	—	—	—
6	1	—	8	—	—	6	—	—	—
7	—	—	5	—	—	3	—	—	—
8	—	—	3	—	—	3	—	—	—
9	—	—	3	—	—	3	—	—	—
10	—	—	3	—	—	2	—	—	—
11	—	—	2	—	—	2	—	—	—
12	—	—	2	—	—	1	—	—	—
13	—	—	1	—	—	1	—	—	—
14	—	—	1	—	—	—	—	—	—
15	—	—	1	—	—	—	—	—	—

The expression values from the 12,488 "genes" on the Affymetrix Mu74Av2 chip were normalized (RMA processing) and averaged between four to six independent datasets. The fold change in expression relative to the control (day 0) was calculated for samples 1, 2, or 3 days after CY treatment. The values in each row are the counts of genes that have a fold change greater than the value at left. The first two columns correspond to genes that are repressed or induced by CY; the last column similarly counts genes in a randomized data group, generated by random permutation of the expression values between individual samples, before normalization and averaging as performed for the true experimental datasets.

represented by a group of genes that are members of the Reg family (Regα, Regγ, and Pap). These pancreas-specific C-type lectins are associated with conditions of pancreatic stress or active growth (e.g., pancreatitis, partial pancreatectomy), but their exact function and origin remains unknown (21–25). All members of the family were induced in a synchronous fashion: a very slight increase at day 1, a dip at day 2, and robust induction at day 3 (Fig. 3*A*). This coordinated response likely denotes a stress response by pancreatic cells, possibly involving cell proliferation in response to the initial noxious effects of the CY-induced decompensation, but also perhaps a reaction to the islet isolation procedure. Overall, however, it is clear that most of the action was taking place in the infiltrate because CY-induced diabetes was not initiated in the target cells themselves.

IFN-γ and the genes it controls dominated the response in a striking manner. The color-coding of the "gene symbol" column of Fig. 3*A*, based on text searches through the cMu74Av2 chip annotation fields and PubMed databases, highlights those genes in which expression is controlled to some extent by IFN-γ. Twenty-five of the 88 genes in the induced set belong to this class (more may also be IFN-γ–responsive, but not yet recognized as such). To some extent, the earlier descriptions of inflammatory changes in CY-induced diabetes did foretell the upregulation of a range of inflammatory cytokines and downstream transcriptional programs (11,14,26,27). Yet, the current data highlight the fact that the effects were very much focused on IFN-γ. Much less prevalent were other inflammatory cytokines that one might have expected to find, such as tumor necrosis factor (TNF)-α or other members of the TNF family. There have been conflicting reports on the importance of IFN-γ in the development of diabetes in the NOD mouse, with different gene ablations of the cytokine or its receptor having contrasting effects in backcrossed animals (28–31). IFN-γ blockade by antibody treatment also had a limited effect on disease (11). The overwhelming impact of IFN-γ uncovered here argues for a reevaluation of this question.

Members of chemokine gene families were among the most strongly induced transcripts. These included Ccl2 and -7 and Cxcl9, -5, and -1. These chemokine transcripts showed parallel profiles of induction, i.e., slightly elevated at day 2, more fully induced at day 3 (Fig. 4*A*), but with a more robust induction for Ccl1 and -5 than for the other chemokine genes. Some of these genes are known to be IFN-γ responsive (but this is not true of all), and their kinetics of induction (contemporary with those of IFN-γ) suggest that other factors might have been responsible for their induction. Interestingly, these induced chemokine genes are clustered in murine genomes, particularly in two regions located on Chr5 and Chr11. Examination of the regions (Fig. 4*B*) shows that the transcriptional activation did not involve the entire cluster, i.e., only some members were induced, whereas others remained silent or unchanged (Figs. 3 and 4*B* and online appendix). Thus, the activation of gene expression did not represent a wholesale activation of chromosomal regions, but rather quite specific effects on particular genes. The disposition of the induced chemokines follows an interesting pattern: in both cases, the most 5′ members of the cluster were those most significantly activated during CY-induced progression to diabetes, whereas there was much less effect on the more distal members of the locus. Is this disposition purely coincidental? It may reflect shared enhancer/response elements, although 130 kb separate Cxcl1 from Cxcl5, which is only 15 kb from the uninduced Cxcl2. It may also reflect the evolutionary history of the loci, inducibility being unequally conferred to duplicated members.

It is important to provide some independent validation of microarray data. In effect, several of the increases had already been validated, since the induction of IL-1α, IL-1β, IFN-γ, and IL-12 have previously been reported (11). In

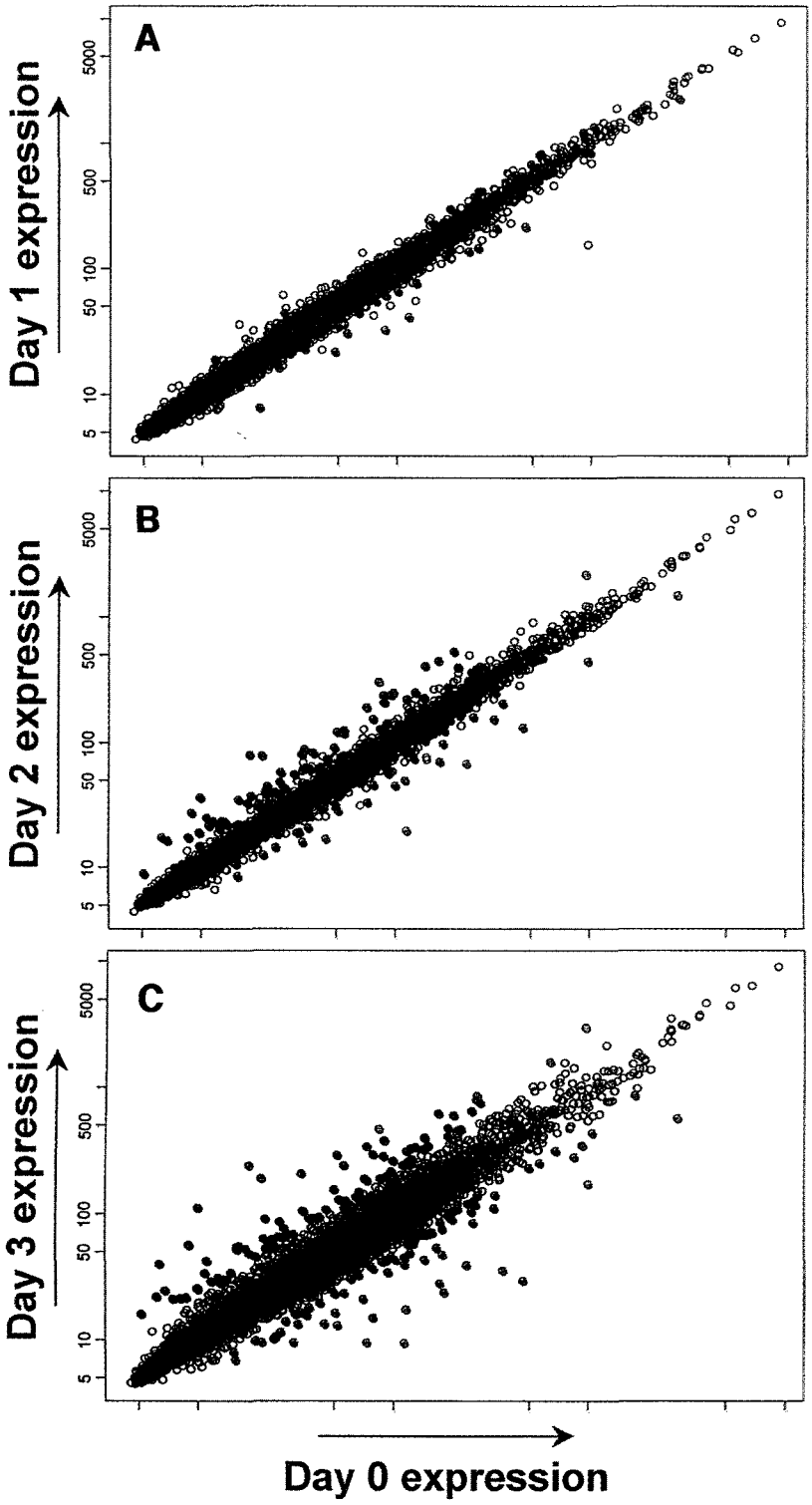

FIG. 2. *A–C*: **Each graph plots the expression level of every gene in the analysis at day 0 on the *x*-axis versus the expression level at day 1, 2, or 3 on the *y*-axis. Genes that demonstrated a progressive increase at day 3 are plotted in red, and those that showed a decrease are plotted in blue.**

addition, we quantitated transcripts of several of the genes belonging to the induced set (Table 3). Transcripts of *IFN-γ* and the *Cxcl9* chemokine (a.k.a. MIG) genes were measured by real-time quantitative analysis (TaqMan). For both genes, the increase detected on the arrays was mirrored in the real-time quantitative PCR analyses. As is commonly observed, the increase in gene expression was scored as greater in the PCR assay than on the microarrays, which tend to underrepresent the degree of variation; thus, the values in Fig. 3 are likely an underestimate of the true range of variation during progression to diabetes.

More generally, the experiments reported here present a broad perspective on gene inductions that accompany CY-induced diabetogenesis. The comparison with PCR data, and in particular with our prior analysis of cytokine induction after CY treatment (11), also illustrates the limitations of the microarray analysis. Several of the genes in which induction was anticipated were indeed members

A

AffyID	Gene Symb.	Gene Title	Locus Link	Chr	Locat. (Mb)	day0	day1	day2	day3	FC d1/d0	FC d2/d0	FC d3/d0	t p-val d3/d0	FPR sims
95348_at	Cxcl1	chemokine (C-X-C motif) ligand 1	14825	5	90.20	18.1	18.2	79.5	239.8	1.00	4.39	13.22	0.00000	5.72E-06
98772_at	Cxcl5	chemokine (C-X-C motif) ligand 5	20311	5	90.06	10.0	11.5	36.1	110.5	1.16	3.63	11.11	0.00001	5.72E-06
95349_g_a	Cxcl1	chemokine (C-X-C motif) ligand 1	14825	5	90.20	20.9	19.7	78.3	188.4	0.94	3.74	9.00	0.00859	5.72E-06
99334_at	Ifng	interferon gamma	15978	10	118.00	6.3	5.8	17.3	39.6	0.91	2.72	6.25	0.19427	5.72E-06
98773_s_at	Irg1	immunoresponsive gene 1	16365	14	94.10	9.0	8.9	27.3	56.1	0.99	3.03	6.23	0.09076	5.72E-06
102877_at	Gzmb	granzyme B	14939	14	46.92	33.4	30.8	80.4	206.0	0.92	2.41	6.16	0.07171	5.72E-06
103202_at	Gbp3	guanylate nucleotide binding protein 3	14469	3	143.22	50.9	51.3	121.1	288.2	1.01	2.38	5.67	0.00238	5.72E-06
96764_at	Iigp1	interferon-inducible GTPase	15945	18	60.59	83.1	84.1	301.6	464.6	1.01	3.63	5.59	0.00000	5.72E-06
93871_at	Il1rn	interleukin 1 receptor antagonist	16181	2	24.62	72.1	79.2	190.1	337.7	1.10	2.64	4.69	0.03796	5.72E-06
94461_at	Pbef	pre-B-cell colony-enhancing factor	18977	12	26.99	55.2	57.4	121.3	239.8	1.04	2.20	4.34	0.00000	1.14E-05
103963_f_a	Iigp1	interferon-inducible GTPase	60440	18	60.62	88.6	87.9	207.9	376.0	0.99	2.35	4.25	0.00618	5.72E-06
160564_at	Lcn2	lipocalin 2	16819	2	32.66	22.1	24.5	39.8	90.4	1.11	1.81	4.10	0.24864	5.72E-06
92315_at	Slfn4	schlafen 4	20558	11	84.00	11.0	11.1	21.5	41.7	1.01	1.95	3.79	0.06919	5.72E-06
100880_at	—	MM diabetic nephropathy-related gene 1 mRNA	18777	3	143.19	77.8	75.0	153.4	292.0	0.97	1.97	3.76	0.01894	5.72E-06
98410_at	Iigp1	interferon-g induced GTPase	15945	11	58.85	168.1	158.2	442.5	615.9	0.94	2.63	3.66	0.00002	5.72E-06
94761_at	Ccl7	chemokine (C-C motif) ligand 7	20306	11	82.83	6.8	6.6	16.3	24.4	0.98	2.41	3.59	0.30202	5.72E-06
99126_at	Xist	inactive X specific transcripts	213742	99	88.39	6.1	5.9	5.6	21.8	0.97	0.91	3.53	0.34170	1.14E-05
103639_at	Ifit3	interferon-induced protein with tetratricopeptide repe	15959	19	33.90	15.8	14.6	34.7	53.9	0.93	2.20	3.42	0.07876	1.14E-05
95621_at	EST	RIKEN cDNA 9030623C06 gene	69835	11	100.27	16.3	18.4	19.4	54.8	1.13	1.19	3.36	0.40230	1.14E-05
98822_at	Isg15	interferon-stimulated protein	15959	4	152.87	26.2	23.4	57.5	85.6	0.90	2.20	3.27	0.10938	1.14E-05
98988_at	Mail	molecule possessing ankyrin-repeats induced by LPS	17389	16	56.08	15.8	18.2	22.0	51.6	1.15	1.39	3.26	0.00002	3.43E-05
102712_at	Saa3	serum amyloid A 3	20210	7	35.36	87.9	60.3	235.1	282.3	0.69	2.68	3.21	0.14668	2.97E-04
103954_at	Reg3a	regenerating islet-derived 3 alpha	19699	6	78.86	266.4	316.4	247.6	846.9	1.19	0.93	3.18	0.26105	5.72E-06
161968_f_a	Ccr5	chemokine (C-C motif) receptor 5	12802	9	124.43	49.3	42.4	90.7	154.0	0.86	1.84	3.12	0.07879	1.14E-05
101800_at	Fpr-rs2	formyl peptide receptor, related sequence 2	14289	17	16.40	10.8	11.0	24.8	33.4	1.02	2.30	3.11	0.20341	5.72E-06
104647_at	Ptgis	prostaglandin-endoperoxide synthase 2	19225	1	150.64	5.1	5.3	8.9	15.9	1.04	1.73	3.10	0.00003	1.14E-05
93078_at	Ly6a	lymphocyte antigen 6 complex, locus A	17067	15	75.20	962.5	855.5	2142.1	2964.0	0.89	2.23	3.08	0.01266	2.29E-05
94556_at	Snx10	sorting nexin 10	71982	6	51.64	34.2	48.5	61.4	104.4	1.42	1.80	3.05	0.00037	1.14E-05
103486_at	Il1b	interleukin 1 beta	16176	2	131.01	34.6	35.1	87.8	103.6	1.01	2.54	2.99	0.18834	5.72E-06
99849_at	—	EST	69835	18	60.62	264.4	409.8	380.8	786.7	1.55	1.44	2.98	0.02819	1.14E-05
97413_at	EST	RIKEN cDNA 1600029D21 gene	76509	9	50.63	17.6	19.6	32.6	52.1	1.11	1.85	2.97	0.08359	5.72E-05
101436_at	Cxcl9	chemokine (C-X-C motif) ligand 9, MIG	17329	5	91.65	202.5	214.6	526.9	595.5	1.06	2.60	2.94	0.00081	5.72E-06
92642_at	Car2	carbonic anhydrase 2	12349	3	14.99	21.7	21.9	39.3	62.8	1.01	1.81	2.90	0.31170	3.43E-05
93096_at	EST	RIKEN cDNA 3010002H13 gene	99571	3	83.95	7.4	7.6	9.9	21.0	1.02	1.33	2.82	0.00010	3.43E-05
104597_at	Gbp2	guanylate nucleotide binding protein 2	14468	3	143.28	142.8	140.5	402.8	397.5	0.98	2.82	2.78	0.06419	5.72E-06
101561_at	Mt2	metallothionein 2	17750	8	93.54	142.5	158.9	189.0	394.0	1.12	1.33	2.77	0.07031	4.58E-05
102995_s_	Gzma	granzyme A	14938	13	109.83	27.6	22.2	42.3	75.8	0.80	1.53	2.75	0.00413	4.58E-05
98628_f_at	Hif1a	hypoxia inducible factor 1, alpha subunit	15251	12	68.60	275.7	338.2	398.4	748.5	1.23	1.45	2.72	0.00592	5.72E-06
99926_at	Pigr	polymeric immunoglobulin receptor	18703	1	131.14	121.0	128.2	177.1	324.8	1.06	1.46	2.69	0.10419	5.72E-05
102873_at	Slc15a2	Peptide transporter 2	19741	17	32.82	115.4	102.0	220.1	308.3	0.88	1.91	2.67	0.13084	5.72E-06
97525_at	Gyk	glycerol kinase	14933	99	70.38	22.6	22.5	31.8	60.3	1.00	1.41	2.67	0.13259	2.29E-05
160646_at	Gsr	glutathione reductase 1	14782	8	32.50	70.4	59.8	94.3	187.2	0.85	1.34	2.66	0.03175	1.14E-05
92715_at	Ubd	ubiquitin D	24108	17	35.82	98.4	102.2	246.8	260.2	1.04	2.51	2.64	0.12958	2.29E-05
92925_at	Cebpb	CCAAT/enhancer binding protein (C/EBP), beta	12608	2	169.56	8.1	7.2	10.5	21.2	0.89	1.30	2.62	0.02719	5.72E-05
94192_at	Gdap10	ganglioside-induced differentiation-associated-protein	14546	12	26.97	18.4	16.3	37.3	48.0	0.89	2.03	2.62	0.28101	6.86E-05
98088_at	Cd14	CD14 antigen	12475	18	37.00	127.8	141.3	248.1	332.8	1.11	1.94	2.60	0.08826	6.86E-05
103258_at	Ly75	DEC 205, CD205	17075	2	61.10	24.1	25.3	29.4	62.0	1.05	1.22	2.58	0.00432	1.14E-05
94774_at	Ifi202	Mouse 202 interferon-activatable protein	26387	1	174.74	9.9	12.1	19.0	25.4	1.22	1.92	2.57	0.11888	3.43E-05
98629_f_at	Hif1a	hypoxia inducible factor 1, alpha subunit	15251	12	68.60	249.9	310.1	357.7	642.3	1.24	1.43	2.57	0.01063	1.14E-05
95908_at	Klra1	killer cell lectin-like receptor, subfamily A, member 1	16641	6	131.26	9.9	8.1	14.7	25.1	0.82	1.48	2.53	0.03833	2.29E-05
94489_at	Ptp4a1	protein tyrosine phosphatase 4a1, PRL-1	19241	1	31.29	72.2	90.4	89.3	182.3	1.25	1.24	2.53	0.01898	5.72E-06
103446_at	EST	RIKEN cDNA 9130009C22 gene	71586	2	63.42	25.9	30.3	48.0	65.0	1.17	1.86	2.51	0.02613	5.72E-06
92558_at	Vcam1	vascular cell adhesion molecule 1	22329	3	116.56	189.1	296.6	275.8	471.6	1.57	1.46	2.49	0.03074	5.72E-06
98833_at	Mmp3	matrix metalloproteinase 3	17392	9	7.43	11.6	18.8	23.3	28.7	1.62	2.01	2.48	0.02811	2.29E-05
94755_at	Il1a	interleukin 1 alpha	16175	2	130.95	8.7	10.3	17.3	21.5	1.18	1.99	2.48	0.20596	6.86E-05
96009_s_a	Pap	pancreatitis-associated protein, Reg3b	19698	6	78.85	633.6	686.3	768.0	1569.1	1.08	1.21	2.48	0.00363	5.72E-05
96042_at	Sod2	superoxide dismutase 2, mitochondrial	20656	17	12.19	37.1	37.6	61.2	91.0	1.01	1.65	2.46	0.03320	4.58E-05
94375_at	Hk2	hexokinase 2	15277	6	83.19	12.6	12.2	20.3	30.7	0.97	1.62	2.45	0.25581	9.15E-05
98000_at	Ly64	lymphocyte antigen 64	17068	16	33.61	52.4	67.8	49.1	127.8	1.29	0.94	2.44	0.37093	5.72E-06
102736_at	Ccl2	chemokine (C-C motif) ligand 2, MCP-1	20296	11	82.82	38.5	40.5	82.0	92.0	1.05	2.13	2.39	0.20568	2.29E-05
160648_at	Fgnl1	fidgetin-like 1	66530	11	11.88	28.1	21.0	32.1	67.0	0.75	1.14	2.38	0.01047	2.29E-05
101465_at	Stat1	signal transducer and activator of transcription 1	20846	1	52.75	45.2	45.7	73.4	107.0	1.01	1.62	2.37	0.01688	1.14E-05
92832_at	Socs1	suppressor of cytokine signaling 1	12703	16	10.27	22.3	19.6	44.4	52.3	0.88	1.99	2.34	0.21062	1.37E-04
99178_at	Gpm6b	glycoprotein m6b	14758	99	146.37	24.2	28.1	25.9	56.5	1.16	1.07	2.34	0.28817	9.15E-05
103816_at	F11r	F11 receptor, Jam	16456	1	172.21	54.0	62.0	73.7	126.1	1.15	1.36	2.33	0.03113	4.58E-05
161642_f_a	Reg3a	regenerating islet-derived 3 alpha	19699	6	78.86	148.5	155.2	125.0	341.6	1.05	0.84	2.30	0.29305	5.72E-05
94792_at	EST	IMAGE AI447305	69835	8	38.56	24.4	28.4	39.6	56.2	1.16	1.62	2.30	0.00170	5.72E-05
160469_at	Thbs1	thrombospondin 1	21825	2	119.74	14.7	17.7	17.2	33.6	1.21	1.17	2.28	0.01854	2.29E-05
98092_at	Plac8	placenta-specific 8	69835	5	97.60	141.2	128.7	225.2	320.9	0.91	1.60	2.27	0.28094	6.86E-05
95848_at	EST	RIKEN cDNA 2900097C17 gene	347740	15	90.10	19.9	7.8	31.0	45.0	0.39	1.56	2.27	0.52869	5.72E-06
162206_f_a	Socs3	suppressor of cytokine signaling 3	12703	11	118.80	41.7	41.3	63.5	93.2	0.99	1.52	2.23	0.03787	6.86E-05
98067_at	Cdkn1a	p21 WAF, cyclin-dependent kinase inhibitor 1A	12575	17	27.81	55.3	56.6	124.7	123.3	1.02	2.26	2.23	0.24846	2.75E-04
160933_at	Ifi47	interferon gamma induced GTPase	15944	11	58.84	95.9	87.3	238.4	213.8	0.91	2.49	2.23	0.02260	5.72E-06
98018_at	Procr	protein C receptor, endothelial	19124	2	157.60	30.7	30.1	55.3	68.4	0.98	1.80	2.23	0.04890	8.01E-05
103754_at	EST	RIKEN cDNA 1100001F19 gene	69835	3	136.09	56.8	58.1	58.4	126.1	1.02	1.03	2.22	0.12937	1.14E-05
104114_at	EST	RIKEN cDNA 2310050N11 gene	66967	1	152.37	66.4	60.6	70.4	147.4	0.91	1.06	2.22	0.22089	1.14E-05
94255_g_a	Clic4	chloride intracellular channel 4 (mitochondrial)	29876	4	133.28	84.8	92.9	127.8	188.2	1.10	1.51	2.22	0.00010	4.58E-05
98077_at	Snrpd3	small nuclear ribonucleoprotein D3	69835	10	75.31	13.6	11.8	15.4	29.8	0.87	1.13	2.19	0.03675	5.72E-05
99183_at	Ppp3r1	protein phospatase 3, regulatory subunit B, alpha iso	69835	11	17.28	117.3	100.5	128.6	256.8	0.86	1.10	2.19	0.00311	2.29E-05
95951_at	Clecsf8	C-type lectin, macrophage, sf8	17474	6	124.23	12.9	12.3	23.3	28.0	0.96	1.81	2.17	0.13098	9.15E-05
93956_at	Ifit3	interferon-induced protein with tetratricopeptide repe	15959	19	33.93	13.7	13.3	22.0	29.6	0.97	1.61	2.16	0.25852	2.75E-04
160277_at	Stxl2	syntaxin 12	100226	4	130.91	123.5	129.6	160.5	265.8	1.05	1.30	2.15	0.00554	3.43E-05
96064_at	Reg3g	regenerating islet-derived 3 gamma	19698	6	78.94	110.8	151.2	97.9	238.4	1.36	0.88	2.15	0.02727	1.14E-05
98405_at	Spi6	serine protease inhibitor 6	20723	13	32.50	91.3	91.0	141.3	195.7	1.00	1.55	2.14	0.04986	1.14E-05
96336_at	Gatm	glycine amidinotransferase (L-arg:gly amidinotransfer	67092	2	124.20	188.9	235.2	243.0	404.1	1.25	1.29	2.14	0.08716	8.01E-05
102401_at	Irf1	interferon regulatory factor 1	16362	11	54.37	212.8	205.1	393.1	454.6	0.96	1.85	2.14	0.12652	4.58E-05

FIG. 3. Genes with significant changes in expression levels between day 0 and day 3. Genes are ordered by fold change from day 0 to day 3 (FC d3/d0) from most to least changed. In the "Locus Link" column, genes expressed predominantly by infiltrating hematopoietic cells are highlighted in green, and genes expressed by pancreatic cells are highlighted in red. *A*: Genes with >2.1-fold increases in gene expression are listed. In the "Gene Symb." column, IFN-γ and those genes in which expression is known to be affected by IFN are highlighted in orange. In the "Gene Title" column, chemokines are highlighted in yellow. *B*: Genes with changes in expression on day 3 versus day 0 of <0.54-fold are listed. In the "Locus Link" column, those genes expressed specifically in B-cells are highlighted in dark green.

B

AffyID	Gene Symb.	Gene Title	Locus Link	Chr	Locat. (Mb)	day0	day1	day2	day3	FC d1/d0	FC d2/d0	FC d3/d0	t p-val. d3/d0	FPR sims
101870_at	Igg1	immunoglobulin heavy chain 4 (serum IgG1)		12	107.39	460.7	214.3	131.7	29.3	0.47	0.29	0.06	0.01087	5.72E-06
102823_at	Igg2b	immunoglobulin IgG2b		12	107.36	113.2	115.5	49.5	9.4	1.02	0.44	0.08	0.00414	5.72E-06
100583_at	Igh-VJ558	immunoglobulin heavy chain (J558 family)		12	107.32	362.8	394.2	204.4	35.2	1.09	0.56	0.10	0.00597	5.72E-06
102824_g_	Igg2b	immunoglobulin IgG2b		12	107.36	73.0	79.9	32.9	9.5	1.09	0.45	0.13	0.00561	5.72E-06
99420_at	IgA	Immunoglobulin IgA		12	107.32	181.4	205.4	123.4	23.5	1.13	0.68	0.13	0.00724	5.72E-06
101869_s_	Hbb-b1	hemoglobin, beta adult major chain		7	92.28	115.4	40.9	19.5	17.3	0.35	0.17	0.15	0.11885	2.29E-05
102372_at	Igj	immunoglobulin joining chain		5	87.79	172.0	161.9	70.1	27.8	0.94	0.41	0.16	0.02277	5.72E-06
92858_at	Slpi	secretory leukocyte protease inhibitor		2	166.22	236.0	136.6	67.6	38.8	0.58	0.29	0.16	0.00823	1.14E-05
102156_f_	Igk-C	IgK chain gene, C-region		6	71.15	990.3	847.5	440.6	170.7	0.86	0.45	0.17	0.00097	1.14E-05
101331_f_	Igk-V8	immunoglobulin kappa chain variable 8 (V8)		6	70.55	78.5	54.6	45.4	14.9	0.70	0.58	0.19	0.00460	5.72E-06
93086_at	Igk-V8	immunoglobulin kappa chain variable 8 (V8)		6	71.15	2829.3	2253.6	1467.6	564.7	0.80	0.52	0.20	0.00017	5.72E-06
100721_f_	IgG Vh+L	scFv Immunoglobulin H+L		6	68.95	51.8	43.8	28.1	12.9	0.85	0.54	0.25	0.00166	3.43E-05
101012_at	Cd79b	CD79B antigen		11	107.16	178.5	125.8	97.1	47.0	0.70	0.54	0.26	0.01442	5.72E-06
101329_f_	Igk-V8	immunoglobulin kappa chain variable 8 (V8)		6	68.75	44.5	34.9	16.9	13.3	0.79	0.38	0.30	0.01780	2.29E-05
98033_at	EST	RIKEN cDNA 1100001H23 gene		6	136.93	143.7	155.1	103.3	42.8	1.08	0.72	0.30	0.00396	4.58E-05
100566_at	Igfbp5	insulin-like growth factor binding protein 5	16011	1	73.50	69.8	70.2	50.1	21.0	1.01	0.72	0.30	0.00414	5.72E-05
93638_s_a	Igl-V1	immunoglobulin lambda chain, variable 1		16	18.54	31.0	24.7	24.5	9.4	0.80	0.79	0.30	0.05630	2.29E-05
95030_at	Prlr	prolactin receptor	19116	15	10.21	166.6	195.3	124.9	53.3	1.17	0.75	0.32	0.00159	5.72E-05
97563_f_at	IgH-V	Immunoglobulin heavy chain gene CDR3		12	109.43	50.4	42.7	29.7	16.2	0.85	0.59	0.32	0.00024	3.43E-05
93583_s_a	IgM	immunoglobulin heavy chain 6 (heavy chain of IgM)		12	107.47	255.6	218.9	158.5	84.0	0.86	0.62	0.33	0.00199	3.43E-05
101054_at	Ii	Ia-associated invariant chain, CD74		18	61.18	841.0	855.3	723.0	278.6	1.02	0.86	0.33	0.01387	3.43E-05
92316_f_at	Igl-V	Ig lambda V region		16	18.95	327.2	207.4	152.9	109.6	0.63	0.47	0.33	0.01323	1.03E-04
103040_at	Cd83	CD83 antigen		13	43.28	113.4	111.7	82.8	39.3	0.99	0.73	0.35	0.02771	1.03E-04
93106_i_at	Tcrb-J	T-cell receptor beta, joining region		6	41.52	93.4	88.3	56.5	34.1	0.95	0.61	0.36	0.15684	1.60E-04
92880_at	Mfge8	milk fat globule-EGF factor 8 protein	17304	7	67.46	925.6	1112.2	841.0	344.0	1.20	0.91	0.37	0.00265	4.58E-05
95356_at	Apoe	apolipoprotein E	11816	7	14.14	920.5	1211.8	1018.6	345.4	1.32	1.11	0.38	0.01017	1.14E-05
104093_at	Lsp1	lymphocyte specific 1		7	131.83	113.6	91.5	83.4	44.5	0.81	0.73	0.39	0.00512	1.26E-04
93584_at	IgM	immunoglobulin heavy chain 6 (heavy chain of IgM)		12	107.47	121.7	97.8	82.3	48.8	0.80	0.68	0.40	0.01757	2.63E-04
93904_f_at	IgH-V (J55	immunoglobulin heavy chain V region (J558 family)		12	108.19	32.6	24.4	19.0	13.1	0.75	0.58	0.40	0.00009	4.58E-05
104564_at	Scg3	secretogranin III		9	75.93	251.2	373.0	232.5	102.7	1.49	0.93	0.41	0.01896	5.72E-05
100376_f_	IgH-V (J55	immunoglobulin heavy chain V region (J558 family)		12	108.19	24.7	17.0	14.4	10.1	0.69	0.58	0.41	0.00288	2.52E-04
102296_at	Pcsk2	proprotein convertase subtilisin/kexin type 2		2	145.51	1039.1	1347.9	987.7	431.5	1.30	0.95	0.42	0.00176	5.72E-05
99823_r_at	EST	DNA segment, Chr 18, ERATO Doi 232, expressed	52492	18	21.18	55.9	30.3	48.9	23.3	0.54	0.88	0.42	0.23272	2.29E-05
92593_at	Osf2	osteoblast specific factor 2 (fasciclin I-like)	50706	3	54.56	25.1	35.0	18.3	10.5	1.40	0.73	0.42	0.06765	4.12E-04
93972_at	Ndufs2	NADH dehydrogenase (ubiquinone) Fe-S protein 2		1	171.98	331.0	385.7	248.1	138.8	1.17	0.75	0.42	0.00114	2.29E-04
95016_at	Nrp	neuropilin		8	128.16	177.8	220.5	147.8	75.0	1.24	0.83	0.42	0.00298	6.86E-05
94781_at	Hba-a1	hemoglobin alpha, adult chain 1		11	32.45	101.0	65.3	45.1	42.9	0.65	0.45	0.42	0.02935	1.94E-04
100362_f_	IgH-V (J55	immunoglobulin heavy chain V region (J558 family)		12	109.80	36.2	31.7	20.7	15.5	0.88	0.57	0.43	0.00656	8.12E-04
99197_at	Gc	group specific component		5	88.72	26.6	43.5	23.4	11.5	1.63	0.88	0.43	0.00267	6.86E-05
92740_at	Igh-6	Immunoglobulin heavy chain, M isotype		12	107.46	15.6	11.6	8.5	6.9	0.74	0.54	0.44	0.03753	5.03E-04
101684_r_	Srst	Simple-repeat sequence containg transcript, T2		11	81.69	263.7	144.6	235.2	116.6	0.55	0.89	0.44	0.25657	4.58E-05
100682_f_	Igk-V8	immunoglobulin kappa chain variable 8 (V8)		6	68.57	21.4	19.8	12.5	9.5	0.92	0.58	0.44	0.00290	5.72E-04
103357_at	Slc2a2	solute carrier family 2 (facilitated glucose transporter)		3	28.53	158.2	222.7	119.0	70.4	1.41	0.75	0.44	0.04197	3.55E-04
95330_at	G6pc-rs	glucose-6-phosphatase, catalytic, related sequence		2	70.10	560.3	820.8	463.9	249.5	1.47	0.83	0.44	0.12092	1.14E-04
97160_at	Sparc	secreted acidic cysteine rich glycoprotein	20692	11	55.99	200.0	278.5	174.2	89.3	1.39	0.87	0.44	0.02039	1.26E-04
99599_s_a	Ptov1	prostate tumor over expressed gene 1		7	33.49	152.1	154.3	137.5	69.1	1.01	0.90	0.45	0.01091	9.15E-05
93109_f_at	Spil-4	serine protease inhibitor 1-4		12	97.78	153.1	157.0	153.6	69.8	1.03	1.00	0.45	0.00446	4.58E-05
99446_at	CD20	Ms4a1, membrane-spanning 4-domains, subfamily A,		19	10.26	126.3	75.7	74.0	57.8	0.60	0.59	0.46	0.03834	1.32E-03
100360_f_	Igh-4	immunoglobulin heavy chain 4 (serum IgG1)		12	110.25	42.1	41.4	29.8	19.4	0.98	0.71	0.46	0.00373	4.12E-04
92422_at	Chga	chromogranin A		12	96.58	674.3	748.5	568.0	311.1	1.11	0.84	0.46	0.01486	2.17E-04
95893_at	Blk	B lymphoid kinase		14	54.01	50.0	34.6	31.9	23.0	0.69	0.64	0.46	0.00659	5.49E-04
100611_at	Lyzs	lysozyme	17105	10	116.94	492.6	674.3	470.9	227.7	1.37	0.96	0.46	0.02822	1.83E-04
100329_at	Spil-4	serine protease inhibitor 1-4		12	97.87	78.4	80.3	77.0	36.3	1.03	0.98	0.46	0.00543	1.03E-04
103596_at	Dgka	diacylglycerol kinase, alpha		10	128.75	90.8	79.8	64.8	42.3	0.88	0.71	0.47	0.03288	3.20E-04
94906_at	Adh1	alcohol dehydrogenase 1 (class I)	11522	3	138.92	97.6	108.5	81.4	45.6	1.11	0.83	0.47	0.00041	2.75E-04
101576_f_	Spil-2	serine protease inhibitor 1-2		12	97.74	144.2	156.4	143.0	68.0	1.08	0.99	0.47	0.00479	9.15E-05
99562_at	Man2b1	mannosidase 2, alpha B1		8	84.39	194.7	212.1	165.7	92.1	1.09	0.85	0.47	0.01304	2.17E-04
101732_at	---	homolog to Drosophila per		7	98.08	87.1	32.3	81.3	41.3	0.37	0.93	0.47	0.30540	4.58E-05
103501_at	Pura	purine rich element binding protein A	19290	18	36.56	118.5	105.8	109.5	56.8	0.89	0.93	0.48	0.03780	1.14E-04
96971_f_at	IgK VJ	Immunoglobulin Kappa V-J joining		6	69.35	37.1	33.8	25.6	17.8	0.91	0.69	0.48	0.00000	5.83E-04
93915_at	Pou2af1	POU domain, class 2, associating factor 1		9	51.36	33.8	22.8	15.8	16.3	0.68	0.47	0.48	0.06995	3.47E-03
96708_at	P24b	integral type I protein	66111	9	89.49	257.3	371.3	231.0	124.1	1.44	0.90	0.48	0.01466	9.15E-05
99187_f_at	EST	RIKEN cDNA 2010315L10 gene		8	70.42	139.8	132.1	116.1	67.9	0.95	0.83	0.48	0.04477	4.00E-04
96943_at	Gps1	G protein pathway suppressor 1		11	121.67	173.4	177.6	181.8	84.6	1.03	1.05	0.49	0.03424	1.03E-04
104239_at	Phemx	Tssc6 tetraspanin		7	132.06	66.2	55.0	47.8	32.4	0.83	0.72	0.49	0.00924	1.50E-03
98574_at	Prpf8	pre-mRNA processing factor 8		11	76.29	129.0	144.3	122.7	63.3	1.12	0.95	0.49	0.01847	1.26E-04
103412_at	EST	RIKEN cDNA 3732412D22 gene	77569	5	66.08	28.2	30.6	22.1	13.9	1.09	0.78	0.49	0.00044	6.06E-04
96972_f_at	Igk-V8	immunoglobulin kappa chain variable 8 (V8)		6	69.35	76.5	73.3	57.6	37.7	0.96	0.75	0.49	0.00762	4.46E-04
99188_at	EST	RIKEN cDNA 2010315L10 gene		8	70.41	240.7	237.4	198.3	118.7	0.99	0.82	0.49	0.06673	3.32E-04
100081_at	Stip1	stress-induced phosphoprotein 1		19	3.21	19.8	20.2	24.4	9.8	1.02	1.24	0.49	0.03868	5.72E-05
93637_at	Cd5	CD5 antigen, Ly1		19	9.72	60.7	52.5	49.9	30.1	0.86	0.82	0.50	0.00367	2.75E-04
92866_at	H2-Aa	histocompatibility 2, class II antigen A, alpha		17	32.88	1719.3	1707.5	1492.5	855.5	0.99	0.87	0.50	0.02973	6.63E-04
96648_at	Coro1a	coronin, actin binding protein 1A		7	115.42	190.1	141.7	160.0	94.9	0.75	0.84	0.50	0.06326	2.40E-04
100468_g_	Lyl1	lymphoblastomic leukemia		8	83.99	31.6	23.9	18.8	15.8	0.75	0.60	0.50	0.02793	2.17E-04
101078_at	Bsg	basigin, CD147	12215	10	79.53	119.4	133.9	111.7	59.7	1.12	0.94	0.50	0.03088	1.26E-04
161756_at	EST	RIKEN cDNA 4833420N02 gene	67390	11	77.03	48.5	21.6	41.0	24.7	0.45	0.85	0.50	0.33184	9.15E-05
96117_r_at	H13	histocompatibility 13		2	154.39	118.4	123.7	116.1	60.4	1.05	0.98	0.50	0.02935	9.15E-05
101972_at	Kdap	kidney-derived aspartic protease-like protein		7	33.21	213.2	180.1	167.5	109.0	0.85	0.79	0.51	0.01027	5.61E-04
100094_at	Supt5h	suppressor of Ty 5 homolog (S. cerevisiae)		7	19.91	65.0	67.6	64.8	33.5	1.04	1.00	0.51	0.04169	1.83E-04
160789_at	EST	RIKEN cDNA 9530090G24 gene		2	157.55	119.7	131.0	122.8	61.7	1.09	1.03	0.51	0.02238	2.97E-04
96605_at	EST	RIKEN cDNA 0610011I04 gene	66058	6	48.88	200.6	233.6	188.3	103.4	1.16	0.94	0.51	0.03229	2.97E-04
104606_at	Cd52	CD52 antigen		4	132.15	268.3	245.5	211.9	138.4	0.92	0.79	0.51	0.03211	6.18E-04
97008_f_at	IgH-V	immunoglobulin heavy chain variable region		12	108.98	15.3	13.0	10.7	7.9	0.85	0.70	0.51	0.00413	2.92E-03
102940_at	Ltb	lymphotoxin B		17	33.81	132.4	97.9	106.5	69.6	0.74	0.80	0.51	0.03516	5.15E-04

FIG. 3—*Continued.*

of the induced set of the present experiments (e.g., IFN-γ, IL-1α, and IL-1β). On the other hand, several others scored as unchanged (IL-12p35, TNF-α, and Fas; see online appendix). Most of these include genes with modest induction scores by PCR analysis, and it has been our experience that microarray analysis very often (but not always) underestimates the magnitude of induction; this is particularly true when the RMA technique is used for probe-level normalization. Others, such as IL-2, were simply not detected in either condition, likely because of the

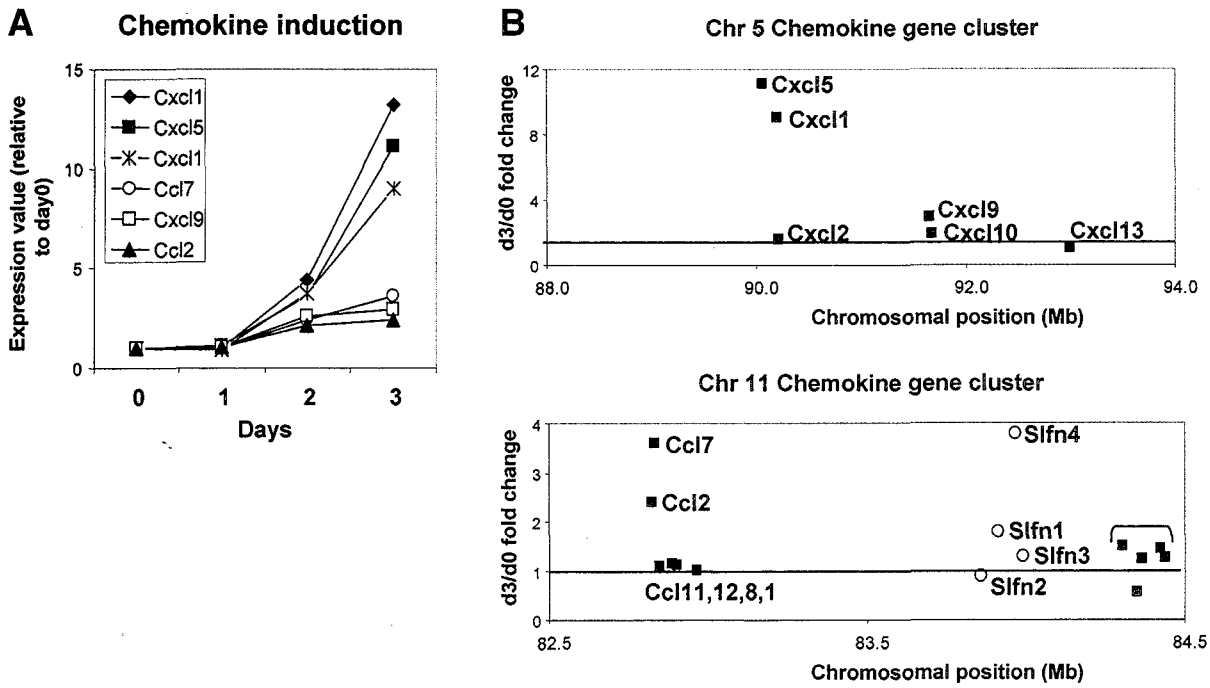

FIG. 4. Chemokine gene induction. *A*: **Fold changes in gene expression at different times during CY induction of diabetes, for six chemokines.** *B*: **Fold changes in gene expression (*y*-axis) are plotted against the position of the genes on chromosome 5 or 11 on the *x*-axis. The position is expressed in Mb, based on the May 2003 release of the public domain sequence of the mouse genome (http://www.ensembl.org/Mus_musculus).**

variable efficacy of oligonucleotide chips. Thus, oligonucleotide chips are powerful tools for revealing broad patterns of coordinate changes, but are of doubtful reliability for quantitating a specific gene product.

Repressed genes. The 84 genes in which transcripts decreased in the 3 days following CY treatment are listed in Fig. 3*B*. They are very different in class and composition from the induced gene set.

A major proportion of the decreased transcripts were genes expressed in B-cells (highlighted in dark green). Twenty-three of the repressed transcripts issued from immunoglobulin loci (heavy or light chains, variable or constant regions) and were among those that showed the most profound reduction, 8 of 10 of the transcripts showing the greatest reduction were from immunoglobulin genes. The reduction was not limited to immunoglobulin genes, a number of other B-cell transcripts were also affected, such as genes encoding molecules involved in antigen presentation (MHC class II, invariant chain), cell surface receptors (CD52, CD79, and CD83), and signal transduction molecules (CD5, Blk, and Dgkα). More than likely, this broad set of decreases reflects a drop in the proportion of B-cells in the insulitic lesion. Insulitis in BDC2.5/NOD mice (and in NOD animals as well) includes a very sizeable proportion of B-cells, which can account for up to 30% of the infiltrate area in immunohistochemical analyses (M.M., R.P., D.M., C.B., unpublished data). CY is known to be particularly toxic to B-cells; treatment with this agent provokes the death of B-cells within 24–48 h after administration (32). Thus, a wave of B-cell death within the infiltrate is likely to be the root of this strong reduction in B-cell–specific transcripts.

As was the case for the induced gene set, only a minority of the "reduced set" transcripts originated from the islet cell compartment. None of those corresponded to the primordial function of pancreatic endocrine cells; in particular, insulin transcripts were only reduced from 6,760 to 6,300 and 5,240 to 4,390 units for *Ins1* and *Ins2*, respectively. This finding indicates that a generalized loss of β-cell function had not yet occurred by 3 days after CY treatment. The transcriptional changes that affected islet cells were predominantly centered on secretory or protease control functions (secretogranin, ChromograninA, Kexin2, and Spi family members), perhaps indicative of early changes in secretory pathways.

Genomic clustering of the CY-induced response. Given the suggestive genomic clustering of the induced chemokine genes, we analyzed more extensively the genomic distribution of those genes in which expression was affected by CY, clustering them according to their chromosomal position (information from the Affymetrix website [NatAffx.com], complemented by BLAST [basic local alignment search tool] searches on the Ensembl genome browser). Genes were considered to potentially belong to a cluster when they mapped <500 kb apart and were either induced or repressed after CY administration. Several interesting clusters were highlighted by this search (Fig. 5). Some were expected, such as the chemokine

TABLE 3
RT-PCR validation of the chip data

Gene	Fold increase (chip)	Fold increase (RT-PCR)
IFN-γ	3.1–10.1	6.9–98
Cxcl9	1.8–4.2	5.9–8.7

The range of observed variation in independent experiments, where the induction of gene transcripts (day 3 relative to day 0) was measured by microarray or by quantitative RT-PCR, is shown.

AffyID	Gene Symbol	Gene Title	Chr	Position (Mb)	day0	day1	day2	day3	d3/d0
[illegible]	[illegible]	NADH dehydrogenase (ubiquinone) Fe-S protein 2	1	171.98	331.0	385.7	248.1	138.8	0.42
[illegible]	[illegible]	F11 receptor, Jam	1	172.21	54.0	62.0	73.7	126.1	2.33
94755_at	Il1a	interleukin 1 alpha	2	130.95	8.7	10.3	17.3	21.5	2.48
103486_at	Il1b	interleukin 1 beta	2	131.01	34.6	35.1	87.8	103.6	2.99
[illegible]	[illegible]	RIKEN cDNA 9530090G24 gene	2	157.55	119.7	131.0	122.8	61.7	0.52
[illegible]	[illegible]	protein C receptor, endothelial	2	157.60	30.7	30.1	55.3	68.4	2.23
100880_at	—	MM diabetic nephropathy-related gene 1 mRNA	3	143.19	77.8	75.0	153.4	292.0	3.76
103202_at	Gbp3	guanylate nucleotide binding protein 3	3	143.22	50.9	51.3	121.1	288.2	5.67
104597_at	Gbp2	guanylate nucleotide binding protein 2	3	143.28	142.8	140.5	402.8	397.5	2.78
[illegible]	[illegible]	chemokine (C-X-C motif) ligand 5	5	90.06	10.0	11.5	36.1	110.5	11.11
[illegible]	[illegible]	chemokine (C-X-C motif) ligand 1	5	90.20	18.1	18.2	79.5	239.8	13.22
[illegible]	[illegible]	chemokine (C-X-C motif) ligand 9, MIG	5	91.65	202.5	214.6	526.9	595.5	2.94
100682_f_a	Igk-V8	immunoglobulin kappa chain variable 8 (V8)	6	68.57	21.4	19.8	12.5	9.5	0.44
101329_f_a	Igk-V8	immunoglobulin kappa chain variable 8 (V8)	6	68.75	44.5	34.9	16.9	13.3	0.30
101331_f_a	Igk-V8	immunoglobulin kappa chain variable 8 (V8)	6	70.55	78.5	54.6	45.4	14.9	0.19
102156_f_a	Igk-C	IgK chain gene, C-region	6	71.15	990.3	847.5	440.6	170.7	0.17
[illegible]	[illegible]	pancreatitis-associated protein, Reg3b	6	78.85	633.6	686.3	768.0	1569.1	2.48
[illegible]	[illegible]	regenerating islet-derived 3 alpha	6	78.86	266.4	316.4	247.6	846.9	3.18
[illegible]	[illegible]	regenerating islet-derived 3 gamma	6	78.94	110.8	151.2	97.9	238.4	2.15
101972_at	Kdap	kidney-derived aspartic protease-like protein	7	33.21	213.2	180.1	167.5	109.0	0.51
99599_s_a	Ptov1	prostate tumor over expressed gene 1	7	33.49	152.1	154.3	137.5	69.1	0.45
[illegible]	[illegible]	lymphoblastomic leukemia	8	83.99	31.6	23.9	18.8	15.8	0.50
[illegible]	Man2b1	mannosidase 2, alpha B1	8	84.39	194.7	212.1	165.7	92.1	0.47
160933_at	Igtp	interferon gamma induced GTPase	11	58.84	95.9	87.3	238.4	213.8	2.23
98410_at	Gtpi-pending	interferon-g induced GTPase	11	58.85	168.1	158.2	442.5	615.9	3.66
[illegible]	[illegible]	chemokine (C-C motif) ligand 2, MCP-1	11	82.82	38.5	40.5	82.0	92.0	2.39
[illegible]	[illegible]	chemokine (C-C motif) ligand 7	11	82.83	6.8	6.6	16.3	24.4	3.59
94192_at	Gdap10	ganglioside-induced differentiation-associated-protein	12	26.97	18.4	16.3	37.3	48.0	2.62
94461_at	Pbef-pending	pre-B-cell colony-enhancing factor	12	26.99	55.2	57.4	121.3	239.8	4.34
[illegible]	Spil-2	serine protease inhibitor 1-2	12	97.74	144.2	156.4	143.0	68.0	0.47
[illegible]	Spil-4	serine protease inhibitor 1-4	12	97.78	153.1	157.0	153.6	69.8	0.46
[illegible]	Spil-4	serine protease inhibitor 1-4	12	97.87	78.4	80.3	77.0	36.3	0.46
100583_at	Igh-VJ558	immunoglobulin heavy chain (J558 family)	12	107.32	362.8	394.2	204.4	35.2	0.10
99420_at	IgA	Immunoglobulin IgA	12	107.32	181.4	205.4	123.4	23.5	0.13
102823_at	IgG2b	immunoglobulin IgG2b	12	107.36	113.2	115.5	49.5	9.4	0.08
101870_at	IgG1	immunoglobulin heavy chain 4 (serum IgG1)	12	107.39	460.7	214.3	131.7	29.3	0.06
97008_f_at	IgH-V	immunoglobulin heavy chain variable region	12	108.98	15.3	13.0	10.7	7.9	0.52
97563_f_at	IgH-V	Immunoglobulin heavy chain gene CDR3	12	109.43	50.4	42.7	29.7	16.2	0.32
100362_f_a	IgH-V (J558	immunoglobulin heavy chain V region (J558 family)	12	109.80	36.2	31.7	20.7	15.5	0.43
[illegible]	[illegible]	immunoglobulin lambda chain, variable 1	16	18.54	31.0	24.7	24.5	9.4	0.30
[illegible]	[illegible]	Ig lambda V region	16	18.95	327.2	207.4	152.9	109.6	0.34
102873_at	Tap2	transporter 2, ATP-binding cassette, sub-family B (MI	17	32.82	115.4	102.0	220.1	308.3	2.67
92866_at	H2-Aa	histocompatibility 2, class II antigen A, alpha	17	32.88	1719.3	1707.5	1492.5	855.5	0.50
[illegible]	[illegible]	purine rich element binding protein A	18	36.56	118.5	105.8	109.5	56.8	0.48
[illegible]	Cd14	CD14 antigen	18	37.00	127.8	141.3	248.1	332.8	2.60
103639_at	Ifit2	interferon-induced protein with tetratricopeptide repe	19	33.90	15.8	14.6	34.7	53.9	3.42
93956_at	Ifit3	interferon-induced protein with tetratricopeptide repe	19	33.93	13.7	13.3	22.0	29.6	2.16

FIG. 5. Clustering of the CY-induced response. Genes in which expression is modified by CY and are located within 500 kb of each other are ordered by chromosomal position. Expression levels at each day and the ratio of expression levels at day 3 to day 0 are shown in the columns to the right.

cluster described above or the immunoglobulin heavy and light chain clusters. The Reg genes also all map within a 140-kb stretch. Others were somewhat of a surprise and may underscore hitherto unrecognized relationships; for example, the "prostate tumor overexpressed gene 1" and "'kidney-derived aspartic protease-like protein" were coordinately repressed and map close to each other on Chr7. Conversely, the genes encoding Pbef and Gdap10 (pre–B-cell colony-enhancing factor and ganglioside-induced differentiation associated protein 10, respectively) map within 20 kb of each other on Chr12 and were induced in concert. Only in one instance did genes in the same geographical cluster respond discordantly, underscoring the significance of the observations, given that random clustering would be expected to generate equal numbers of concordant and discordant clusters.

What pathways are involved? These results paint a broad portrait of the molecular processes participating in progression to diabetes subsequent to treatment of insulitic mice with CY. This progression involves the extinction of B-cell transcripts and induction of a response dominated by IFN-γ and the genes it controls. Interestingly, this pattern has significant but incomplete overlap with that detected when comparing the "respectful" and "destructive" islet infiltrates that develop when the BDC2.5TCR transgene is bred onto different genetic backgrounds (L. Poirot, D.M., C.B., unpublished observations). Overabundant IFN-γ gene expression and overexpression of certain IFN-γ–responsive transcripts were also found in the latter context, whereas other genes highlighted in the present study were not differentially expressed, including the chemokine and Schlafen gene families or the B-cell–derived transcripts. Thus, the various aggressive/destructive forms of insulitis observed under different conditions (CY induced or genetic background influenced) may represent a common cellular phenotype at which different immunoregulatory perturbations converge. IFN-γ and the genes it induces would be at the point of convergence, whether resulting from NK-related overexpression or from chemical induction. IFN-γ would then activate the full cytotoxic potential of the various cell types present in the lesion, i.e., T-cells, but also NK cells or macrophages, or even neutrophils, which are secondarily recruited after CY induction (33).

In the case of CY-induced diabetes, one might speculate that the disappearance of B-cells is at the root of the process, either because B-cell depletion results in the release of large amounts of apoptotic cell fragments, thus activating the myeloid cells that abound in the lesion and altering their capacity to interact with/control T-cells, or because B-cells exert a regulatory influence in and of themselves, as was proposed by Turk (34) in the mid-1970s and more recently in a murine model of arthritis (35). Disappearance of B-cells would unleash, then, aggressive insulitis. Although not usually thought as central to the pathogenesis of type 1 diabetes, B-cells do play an important role, as shown by the quasi-absence of autoimmune attacks in B-cell–deficient NOD mice (36–38), although this point is more controversial in the human milieu (39). This is usually interpreted as a perturbation of antigen presentation, which prevents the initial priming of autoreactive T-cells. The present data lead one to speculate that B-cells may also be involved in later stages of the process, when regulatory balances condition the outcome of the autoimmune lesion.

On the other hand, our data do not support the oft-evoked notion that CY exerts its influence by depleting suppressor T-cells. The aggressiveness of the insulitic lesion in BDC2.5 mice is strongly conditioned by regulatory T-cell populations, which are under the control of costimulatory family genes such as ICOS or CTLA-4 (6,40) (A. Herman, C.B., D.M., unpublished observations). In the latter study, diabetes induced by ICOS blockade correlated with clear changes in the "Treg signature," a set of 150 genes differentially expressed in $CD25^+CD4^+$ regulatory cells (41). In the present data, such changes were conspicuously absent. In addition, we have not observed significant reductions in pancreatic $CD25^+$ T regulatory cells after CY treatment (A. Herman, D.M., C.B., unpublished data). Thus, and unless CY affects a very minor subpopulation with regulatory potential, changes in T regulatory populations do not seem prevalent in CY-induced diabetes.

In conclusion, this analysis reveals a landscape dominated, to a striking degree, by IFN-γ and the genes it controls. The model used here certainly represents an extreme form of β-cell destruction, and it will be important to assess whether IFN-γ occupies such a central position in other instances of autoimmune β-cell destruction, and whether the molecular and cellular pathways uncovered in this mouse system play a role in human patients.

ACKNOWLEDGMENTS

This work was supported by grants from the National Institutes of Health and the JDRF to D.M. and C.B. (P01 AI 39671 and 9-1998-1004), by grants from Joslin's National Institute of Diabetes and Digestive and Kidney Diseases (NIDDK)-funded Diabetes and Endocrinology Research Center (DERC) cores, and by funds from the W.T. Young Chair for Diabetes Research. M.M. was supported by grants from the JDRF and the Endocrine Fellows Foundation.

We thank members of the Benoist-Mathis lab and John Rogus for discussion; Jack O'Neill, Vaja Tchipashvili, and Gordon Weir of the JDRF Center for Islet Transplantation at Harvard's Islet Preparation Core for provision of islets; Robert Saccone of the DERC Microarray Core for processing and hybridization of the probes; and Judy George and Ella Hyatt for maintaining the BDC2.5 colony.

REFERENCES

1. Ohashi PS, Oehen S, Buerki K, Pircher H, Ohashi CT, Odermatt B, Malissen B, Zinkernagel RM, Hengartner H: Ablation of "tolerance" and induction of diabetes by virus infection in viral antigen transgenic mice. *Cell* 65:305–317, 1991
2. Von Herrath MG, Dockter J, Oldstone MB: How virus induces a rapid or slow onset insulin-dependent diabetes mellitus in a transgenic model. *Immunity* 1:231–242, 1994
3. Katz JD, Wang B, Haskins K, Benoist C, Mathis D: Following a diabetogenic T cell from genesis through pathogenesis. *Cell* 74:1089–1100, 1993
4. Verdaguer J, Schmidt D, Amrani A, Anderson B, Averill N, Santamaria P: Spontaneous autoimmune diabetes in monoclonal T cell nonobese diabetic mice. *J Exp Med* 186:1663–1676, 1997
5. Haskins K, Portas M, Bergman B, Lafferty K, Bradley B: Pancreatic islet-specific T-cell clones from nonobese diabetic mice. *Proc Natl Acad Sci U S A* 86:8000–8004, 1989
6. Luhder F, Höglund P, Allison JP, Benoist C, Mathis D: Cytotoxic T lymphocyte-associated antigen 4 regulates the unfolding of autoimmune diabetes. *J Exp Med* 187:427–432, 1998
7. Herman AE, Freeman GJ, Mathis D, Benoist C: Profile of an autoimmune lesion: a balancing act between T effectors and T regulators. *J Exp Med* 199:1479–1489, 2004
8. Ansari M, Salama, Ad, Chitnis T, Smith RN, Yagita H, Akiba H, Yamazaki T, Azuma M, Iwai H, Khoury SJ, Auchincloss H Jr, Sayegh MH: The programmed death-1 (PD-1) pathway regulates autoimmune diabetes in nonobese diabetic (NOD) mice. *J Exp Med* 198:63–69, 2003
9. Balasa B, Van Gunst K, Sarvetnick N: The microbial product lipoploysaccharide confers diabetogenic potential on repertoire of BDC2.5/NOD mice: implications for the etiology of autoimmunity. *Clin Immunol* 95:93–98, 2000
10. Horwitz MS, Bradley LM, Harbertson J, Krahl T, Lee J, Sarvetnick N: Diabetes induced by Coxsackie virus: initiation by bystander damage and not molecular mimicry. *Nat Med* 4:781–785, 1998
11. André-Schmutz I, Hindelang C, Benoist C, Mathis D: Cellular and molecular

changes accompanying the progression from insulitis to diabetes. *Eur J Immunol* 29:245–255, 1999
12. Harada M, Makino S: Promotion of spontaneous diabetes in non-obese diabetes-prone mice by cyclophosphamide. *Diabetologia* 27:604–606, 1984
13. Yasunami R, Bach JF: Anti-suppressor effect of cyclophosphamide on the development of spontaneous diabetes in NOD mice. *Eur J Immunol* 18:481–484, 1988
14. Rothe H, Faust A, Schade U, Kleemann R, Bosse G, Hibino T, Martin S, Kolb H: Cyclophosphamide treatment of female non-obese diabetic mice causes enhanced expression of inducible nitric oxide synthase and interferon-gamma, but not of interleukin-4. *Diabetologia* 37:1154–1158, 1994
15. Gotoh M, Maki T, Kiyoizumi T, Satomi S, Monaco AP: An improved method for isolation of mouse pancreatic islets. *Transplantation* 40:437–438, 1985
16. Gonzalez A, Katz JD, Mattei MG, Kikutani H, Benoist C, Mathis D: Genetic control of diabetes progression. *Immunity* 7:873–883, 1997
17. Luhder F, Chambers C, Allison JP, Benoist C, Mathis D: Pinpointing when T cell costimulatory receptor CTLA-4 must be engaged to dampen diabetogenic T cells. *Proc Natl Acad Sci U S A* 97:12204–12209, 2000
18. Mueller R, Bradley LM, Krahl T, Sarvetnick N: Mechanism underlying counterregulation of autoimmune diabetes by IL-4. *Immunity* 7:411–418, 1997
19. Kanagawa O, Militech A, Vaupel BA: Regulation of diabetes development by regulatory T cells in pancreatic islet antigen-specific TCR transgenic nonobese diabetic mice. *J Immunol* 168:6159–6164, 2002
20. Irizarry RA, Hobbs B, Collin F, Beazer-Barclay YD, Antonellis KJ, Scherf U, Speed TP: Exploration, normalization, and summaries of high density oligonucleotide array probe level data. *Biostatistics* 4:249–264, 2003
21. Baeza N, Sanchez D, Vialettes B, Figarella C: Specific reg II gene overexpression in the non-obese diabetic mouse pancreas during active diabetogenesis. *FEBS Lett* 416:364–368, 1997
22. Sanchez D, Baeza N, Blouin R, Devaux C, Grondin G, Mabrouk K, Guy-Crotte O, Figarella C: Overexpression of the reg gene in non-obese diabetic mouse pancreas during active diabetogenesis is restricted to exocrine tissue. *J Histochem Cytochem* 48:1401–1410, 2000
23. Gurr W, Yavari R, Wen L, Shaw M, Mora C, Christa L, Sherwin RS: A Reg family protein is overexpressed in islets from a patient with new-onset type 1 diabetes and acts as T-cell autoantigen in NOD mice. *Diabetes* 51:339–346, 2002
24. Baeza NJ, Moriscot CI, Renaud WP, Okamoto H, Figarella CG, Vialettes BH: Pancreatic regenerating gene overexpression in the nonobese diabetic mouse during active diabetogenesis. *Diabetes* 45:67–70, 1996
25. Ohno T, Ishii C, Kato N, Ito Y, Shimizu M, Tomono S, Murata K, Kawazu S: Increased expression of a regenerating (reg) gene protein in neonatal rat pancreas treated with streptozotocin. *Endocr J* 42:649–653, 1995
26. Rothe H, Ito Y, Kolb H: Disease resistant, NOD-related strains reveal checkpoints of immunoregulation in the pancreas. *J Mol Med* 79:190–197, 2001
27. Prud'homme GJ, Chang Y: Prevention of autoimmune diabetes by intramuscular gene therapy with a nonviral vector encoding an interferon-gamma receptor/IgG1 fusion protein. *Gene Ther* 6:771–777, 1999
28. Hultgren B, Huang X, Dybdal N, Stewart TA: Genetic absence of γ-interferon delays but does not prevent diabetes in NOD mice. *Diabetes* 45:812–817, 1996
29. Wang B, André I, Gonzalez A, Katz JD, Aguet M, Benoist C, Mathis D: Interferon-γ impacts at multiple points during the progression of autoimmune diabetes. *Proc Natl Acad Sci U S A* 94:13844–13849, 1997
30. Kanagawa O, Xu G, Tevaarwerk A, Vaupel BA: Protection of nonobese diabetic mice from diabetes by gene(s) closely linked to IFN-gamma receptor loci. *J Immunol* 164:3919–3923, 2000
31. Serreze DV, Post CM, Chapman HD, Johnson EA, Lu B, Rothman PB: Interferon-γ receptor signaling is dispensable in the development of autoimmune type 1 diabetes in NOD mice. *Diabetes* 49:2007–2011, 2000
32. Turk JL, Parker D: Effect of cyclophosphamide on immunological control mechanisms. *Immunol Rev* 65:99–113, 1982
33. André I, Gonzalez A, Wang B, Katz J, Benoist C, Mathis D: Checkpoints in the progression of autoimmune disease: lessons from diabetes models. *Proc Natl Acad Sci U S A* 93:2260–2263, 1996
34. Turk JL: The organization of lymphoid tissue in relation to function. *Lymphology* 10:46–53, 1977
35. Mauri C, Gray D, Mushtaq N, Londei M: Prevention of arthritis by interleukin 10-producing B cells. *J Exp Med* 197:489–501, 2003
36. Serreze DV, Chapman HD, Varnum DS, Hanson MS, Reifsnyder PC, Richard SD, Fleming SA, Leiter EH, Shultz LD: B lymphocytes are essential for the initiation of T cell-mediated autoimmune diabetes: analysis of a new "speed congenic" stock of NOD.Ig mu null mice. *J Exp Med* 184:2049–2053, 1996
37. Serreze DV, Fleming SA, Chapman HD, Richard SD, Leiter EH, Tisch RM: B lymphocytes are critical antigen-presenting cells for the initiation of T cell-mediated autoimmune diabetes in nonobese diabetic mice. *J Immunol* 161:3912–3918, 1998
38. Greeley SA, Katsumata M, Yu L, Eisenbarth GS, Moore DJ, Goodarzi H, Barker CF, Naji A, Noorchashm H: Elimination of maternally transmitted autoantibodies prevents diabetes in nonobese diabetic mice. *Nat Med* 8:399–402, 2002
39. Martin S, Wolf-Eichbaum D, Duinkerken G, Scherbaum WA, Kolb H, Noordzij JG, Roep BO: Development of type 1 diabetes despite severe hereditary B-lymphocyte deficiency. *N Engl J Med* 345:1036–1040, 2001
40. Gonzalez A, Andre-Schmutz I, Carnaud C, Mathis D, Benoist C: Damage control, rather than unresponsiveness, effected by protective DX5+ T cells in autoimmune diabetes. *Nat Immunol* 2:1117–1125, 2001
41. McHugh RS, Whitters MJ, Piccirillo CA, Young DA, Shevach EM, Collins M, Byrne MC: CD4(+)CD25(+) immunoregulatory T cells: gene expression analysis reveals a functional role for the glucocorticoid-induced TNF receptor. *Immunity* 16:311–323, 2002